

## Author Manuscript

**Title:** Control of stereoselectivity in diverse hapalindole metabolites is mediated by cofactor induced combinatorial pairing of Stig cyclases

**Authors:** Shasha Li, Ph.D.; Sean A. Newmister, Ph.D.; Andrew N. Lowell; Jiachen Zi; Callie R. Chappell; Fengan Yu; Robert M. Hohlman; Jimmy Orjala; Robert M. Williams; David H. Sherman

This is the author manuscript accepted for publication and has undergone full peer review but has not been through the copyediting, typesetting, pagination and proofreading process, which may lead to differences between this version and the Version of Record.

**To be cited as:** 10.1002/anie.201913686

**Link to VoR:** <https://doi.org/10.1002/anie.201913686>

# Control of stereoselectivity in diverse hapalindole metabolites is mediated by cofactor induced combinatorial pairing of Stig cyclases

Shasha Li, Sean A. Newmister, Andrew N. Lowell, Jiachen Zi, Callie R. Chappell, Fengang Yu, Robert M. Hohlman, Jimmy Orjala, Robert M. Williams, and David H. Sherman\*

**Abstract:** The stereospecific polycyclic core formation of hapalindoles and fischerindoles is controlled by the Stig cyclases through a three-step cascade involving Cope rearrangement, 6-*exo*-trig cyclization and a final electrophilic aromatic substitution. Here we report a comprehensive study of all currently annotated Stig cyclases, and reveal that these proteins can assemble into heteromeric complexes induced by Ca<sup>2+</sup> to cooperatively control the stereochemistry of hapalindole natural products.

## Introduction

After many years of isolation, structural characterization and total synthesis,<sup>[1]</sup> hapalindole-type alkaloids from Stigonematales cyanobacteria have re-gained significant scientific attention due to their pharmacological potential and unique biogenesis. Recent studies have revealed that hapalindole H inhibits NF- $\kappa$ B and has selective cytotoxicity against the PC-3 prostate cancer cell line,<sup>[2]</sup> while 12-*epi*-hapalindole H shows embryo toxicity in vertebrate development.<sup>[3]</sup> Several other hapalindoles appear to be neurotoxins by modulating sodium channels in human cells.<sup>[4]</sup> A growing focus from several research groups involves the elucidation of the biosynthetic mechanism of these alkaloids,<sup>[5]</sup> specifically their stereo- and regiochemically diverse polycyclic ring formation,<sup>[6]</sup> which results in six stereochemical patterns based on the C10, C11, C12, and C15 chiral centers (**Figure 1**). We recently reported a novel class of Stig cyclases that specify hapalindole and fischerindole formation from the central C3-geranylated cis-indole isonitrile intermediate (**1**, **Figure 1**,

**Figure S1**).<sup>[5a]</sup> This class of enzyme catalyzes a coupled Cope rearrangement/ring-forming cascade and elaborates the four chiral centers and three types of ring systems.<sup>[6a]</sup> Considerable recent progress has been made toward a mechanistic understanding of these core assembly reactions through a crystal structure of the HpiC1 cyclase and computational modeling of the three-part reaction scheme.<sup>[7]</sup> However, further studies of these remarkable biocatalysts are required to fully understand the basis for stereochemical control during assembly of diverse hapalindole and fischerindole metabolites.

In a previous report,<sup>[6a]</sup> we characterized several Stig cyclases, including FamC1 and its homologs FilC1/HpiC1 that generate 12-*epi*-hapalindole U (**3a**), FimC5/FisC generating 12-*epi*-fischerindole U (**3c**), and the heterodimeric combination FamC2-FamC3 generating hapalindole H (**4a**) (**Figure 1**). Phylogenetic analysis was applied to predict the product profile of Stig cyclases based on the rationale that proteins with high sequence identity will produce the same or highly similar metabolites.<sup>[6a]</sup> In addition, we demonstrated that Stig cyclases function as homodimeric (e.g. FamC1) or heterodimeric (e.g. FamC2-FamC3) complexes to generate stereochemically distinct products. These results provided an initial characterization of the stereoselectivity and regioselective divergence for C-ring coupling between hapalindoles and fischerindoles.

In the current study, we sought to decrypt the basis for stereoselectivity among all six naturally observed stereochemical patterns identified from over 30 years of studies involving direct isolation of metabolites from wild type cyanobacterial strains.<sup>[1b, 3]</sup> These studies provide a new, nuanced biochemical understanding of the Stig cyclases, and reveal a natural system for combinatorial biocatalytic diversification in these pathways.

## Results and Discussion

The course of our studies described here was developed upon noticing a mismatch in reported metabolites from the ambigueine-producing strain *Fischerella* sp. IL 199-3-1 (*fil*),<sup>[8]</sup> and product prediction from its Stig cyclases based on phylogenetic analysis. The *fil* gene cluster contains four Stig cyclases (FilC1-C4), which share high sequence similarities to FamC1-C4 from *Fischerella ambigua* UTEX 1903. We demonstrated previously that FilC1 is a FamC1 functional homolog and catalyzes formation of 12-*epi*-hapalindole U (**Figure 2**).<sup>[6a]</sup> While both FilC2 and FilC3 are 98% identical to FamC2 and FamC3, respectively, they were expected to produce hapalindole H (**4a**). However, the isolated metabolites from cultured IL 199-3-1 contains 12-*epi*-hapalindole H (**5a**, C10*R*, 11*R*, 12*S*, and 15*R*) instead of hapalindole H (**4a**, C10*R*, 11*R*, 12*R*, and 15*R*) (**Figure S2**).<sup>[8-9]</sup> Because of this discordance with expectations, we decided to address whether FilC2-FilC3 behaves differently from FamC2-FamC3 to produce

\*]Prof. D. H. Sherman  
Life Sciences Institute, Department of Medicinal Chemistry,  
Chemistry, Microbiology & Immunology  
The University of Michigan  
210 Washtenaw Avenue, Ann Arbor, MI 48109-2216n(USA)  
davidhs@umich.edu

Dr. S. Li, R. M. Hohlman  
Life Sciences Institute, Department of Medicinal Chemistry  
Dr. A. Lowell, Dr. S. Newmister, Dr. F. Yu  
Life Science Institute  
C. R. Chappell  
Department of Molecular, Cellular & Developmental Biology  
The University of Michigan  
210 Washtenaw Avenue, Ann Arbor, MI 48109-2216n(USA)  
Prof. J. Orjala, Dr. J. Zi  
Department of Pharmaceutical Sciences  
College of Pharmacy  
University of Illinois at Chicago  
Chicago, Illinois 60612 (USA)  
Prof. R. M. Williams  
Department of Chemistry  
Colorado State University, Fort Collins, CO 80523  
University of Colorado Cancer Center, Aurora, CO 80045

Supporting information for this article is given via a link at the end of the document.

**5a** instead of **4a** despite such high sequence identities. Thus, we generated FilC2 and FilC3 in *E. coli* and analyzed the products of the in vitro reaction.

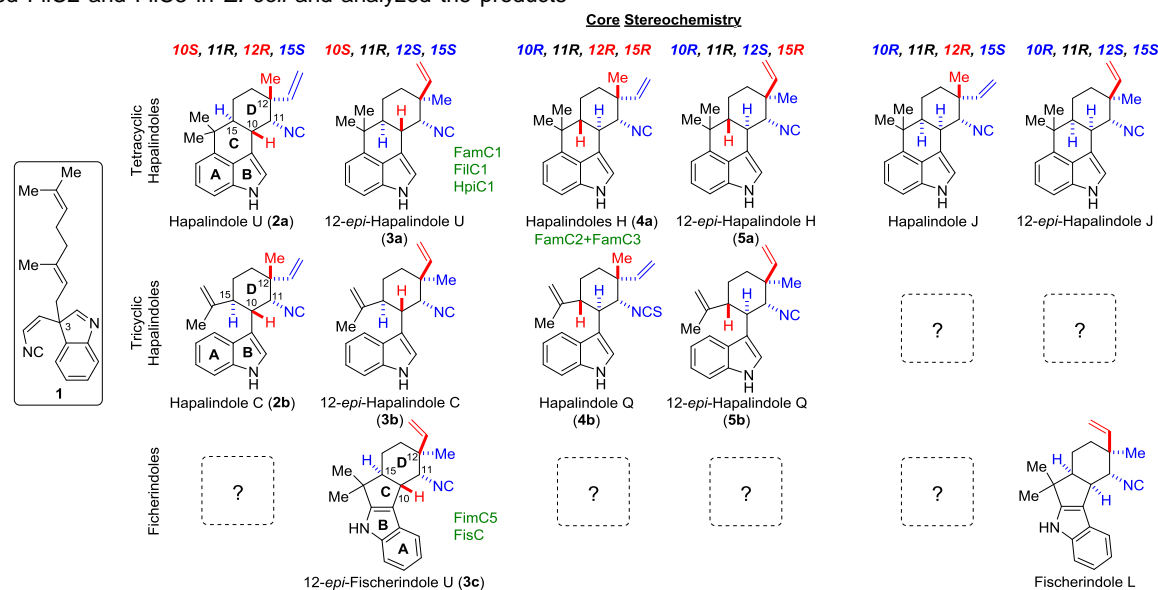


**Figure 1.** Stereochemical classification of hapalindole and fischerindole metabolites based on C10, C11, C12, and C15 stereocenters. All chemical patterns were discovered from nature, except 12-*epi*-hapalindole U (**3a**) which was initially identified from in vitro chemoenzymatic assay,<sup>[5a]</sup> however, its stereo pattern has been observed in 12-*epi*-ambiguine B nitrile.<sup>[3]</sup> Dashed-line boxes with a question mark represent stereochemical configurations that are predicted, but remain unidentified as isolated natural products. The characterized Stig cyclases are shown adjacent its (major) products (green text).

In this experimental system, FilC2 and FilC3 were almost completely inactive both as a pair and as individual proteins, in contrast to FamC2 and FamC3, which together produce **4a** in a heterodimeric form.<sup>[6a]</sup> Based on our hypothesis that a missing cellular component was required for activity, the cell-free lysate of *Fischerella sp.* IL 199-3-1 was introduced into the reaction mixture and facile conversion of substrate **1** was observed (**Figure 2**). Furthermore, we found that BG-11 culture broth alone, a metal-rich medium used for cyanobacterial cultivation, is sufficient to stimulate the activity. Additional screening with the metal components in BG-11 broth revealed that supplemental calcium chloride and magnesium chloride promoted the reaction, with Ca<sup>2+</sup> exhibiting the highest efficiency (**Figure 2, Figure S4**). To characterize the structure of the FilC2-FilC3 derived metabolites, we conducted a large-scale in vitro reaction using intermediate **1** with 5 mM of CaCl<sub>2</sub> and isolated the products for NMR analysis. Under these conditions, the major compound was identified as 12-*epi*-hapalindole H **5a** (**Figure S5 and SI Table 2**), which is consistent with its isolation from cultured *Fischerella sp.* IL 199-3-1.<sup>8</sup> Thus, we confirmed that despite FilC2/FilC3 being 98% identical to the FamC2/FamC3 system, a metabolite **5a** with alternative C-12 stereochemistry (compared to hapalindole H **4a**)<sup>[6a, 9b]</sup> was produced. Minor products were also isolated, two of which we identified as tricyclic variants 12-*epi*-hapalindole C (**3b**)<sup>[6a]</sup> and 12-*epi*-hapalindole Q (**5b, Figure S6**)<sup>[10]</sup>.

The FilC2-FilC3 pair was the first example in our investigation that required excess Ca<sup>2+</sup> for function and resulted in formation of different metabolites compared to their most closely related Stig cyclase homologs. To assess the effect of Ca<sup>2+</sup> on metabolite stereochemical configuration, we compared the

products of FamC2-FamC3 and other previously characterized Stig cyclases<sup>[6a]</sup> after introduction of excess Ca<sup>2+</sup>, and found that these metabolite profiles remained unchanged. While all reactions could be suppressed by adding EDTA, we confirmed that Ca<sup>2+</sup> is a key component for functional Stig cyclases. In addition to maintaining structural and functional integrity,<sup>[7a]</sup> it is now evident that excess Ca<sup>2+</sup> plays another important role in FilC2-FilC3, a realization that motivated further detailed studies.

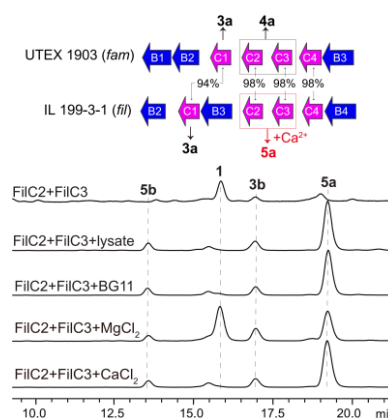


**Figure 2.** FilC2 and FilC3 functional assay with excess calcium (5 mM) leading to 12-*epi*-hapalindole H (**5a**). [Note: all reactions in this report were conducted with 5 mM of calcium chloride unless otherwise noted.]

We proceeded by testing individual Stig cyclases with excess Ca<sup>2+</sup> and found that it activates FilC2 to produce the same

metabolites observed when paired with FilC3, albeit at reduced levels. By contrast, even with excess  $\text{Ca}^{2+}$ , FilC3 and FamC3 remained catalytically inactive in the absence of FilC2 and FamC2, respectively. Surprisingly, FamC2 alone generated 12-*epi*-hapalindole H (**5a**) instead of hapalindole H (**4a**), the product of heterodimeric FamC2-FamC3 (**Figure 3**, **Figure S7**). This observation compelled us to reconsider the role of FamC3 in controlling the stereochemistry at C-12 during hapalindole assembly. Based on the high degree of similarity between FamC3 and FilC3, we decided to investigate the heterologous cross-pairing of FamC2-FamC3 and FilC2-FilC3 (**Figure 3**). We found that pairing of FamC2-FilC3 resulted in production of 12-*epi*-hapalindole H **5a**, identical to the product obtained with FamC2 alone. However, pairing of FilC2-FamC3 resulted in formation of hapalindole H **4a**, different from FilC2-FilC3, which was further shown by  $^1\text{H}$  NMR analysis to be a 4:1 mixture of **4a** and **5a** (**Figure S8**). Two of the three minor products were confirmed to be tricyclic hapalindole C (**2b**, **Figure S9**) and 12-*epi*-hapalindole C (**3b**). Similar results were observed in another homologous pair HpiC2 (99% identical to FamC2) and HpiC3 (100% identical to FamC3 of the first 198/202 amino acids),<sup>[6a]</sup> where HpiC3 can modulate the reaction outcome from the expected 12-*epi*-hapalindole H product of HpiC2/FamC2 to hapalindole H (**Figure S10**). This result suggests that FamC3/HpiC3 may actively control the stereochemistry of hapalindoles, while FilC3 does not exert similar control.

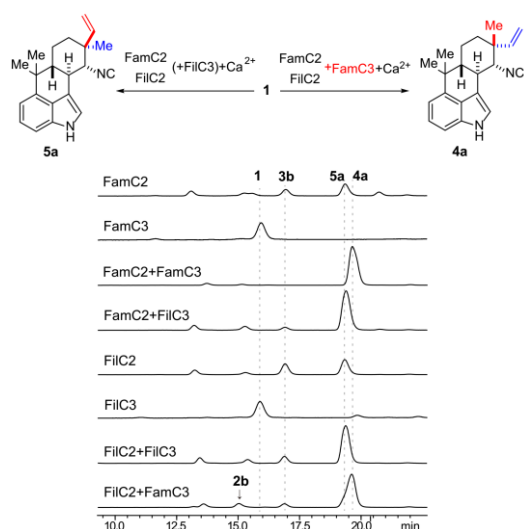


**Figure 3.** In vitro analysis of FamC2/FamC3, FilC2/FilC3 and their heterologous cross-pairing, with 5 mM  $\text{CaCl}_2$ .

This product profile reconfiguration was also observed in our investigation of another hapalindole/ambiguine-producing strain *Westiellopsis prolifica* SAG 16.93 (*wep*), which also showed a discrepancy between metabolites isolated from the cyanobacterium, and products predicted from Stig cyclase sequence comparisons. This strain is known to produce hapalindole U and hapalindole H (**Figure S3**), but only two Stig cyclases were identified in the *wep* gene cluster, denoted as WepC1 and WepC2. WepC1 was classified as a FamC1

homolog based on 89% sequence identity, while WepC2 is a FamC4 homolog with 93% identity. Despite observed production of hapalindole H by this strain, no FamC2/FamC3 homologs were identified from the *wep* cluster or from analysis of the broader genome sequence (**Figure 4**). In vitro assays demonstrated that WepC1 behaves similarly to FamC1 by producing 12-*epi*-hapalindole U **3a** as the major metabolite, in addition to low levels of tricyclic 12-*epi*-hapalindole C **3b** (10%). WepC1 differs from FamC1 in that it requires excess  $\text{Ca}^{2+}$  for activity. WepC2 was inactive (similar to FamC4), both with and without excess calcium. Thus, after analyzing both cyclases individually, neither of them generated the hapalindoles isolated from *W. prolifica* SAG 16.93. Inspired by our finding with FilC2-FilC3, we combined WepC1 and WepC2 in 1:1 ratio with 5 mM of  $\text{CaCl}_2$ , and the product profile was completely altered. Instead of **3a**, the WepC1-WepC2 heteromeric combination produced three new metabolites (**Figure 4**), characterized through NMR analysis to be hapalindole U (**2a**, C10S, 11R, 12R, and 15S), tricyclic hapalindole C **2b** (5:1 ratio, **Figure S11**), and trace level of hapalindole H **4a**.

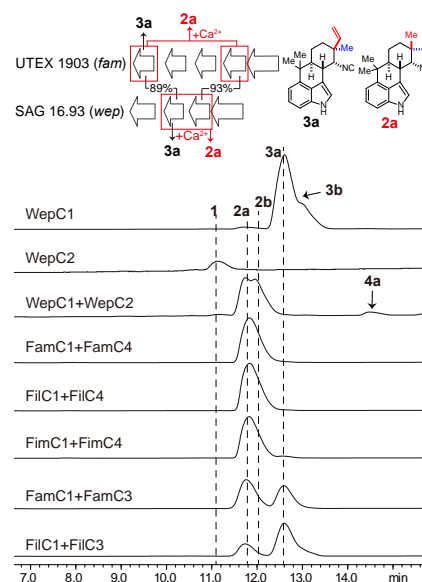


**Figure 4.** In vitro analysis of WepC1 and WepC2 and homologs for production of hapalindole U (**2a**) with 5 mM  $\text{CaCl}_2$ .

The discovery of product profile reconfiguration induced by heteromeric pairing of Stig cyclases inspired us to track the hapalindole U producer. Except 12-*epi*-ambiguine nitrile,<sup>[3]</sup> all other isolated ambiguines share the same stereochemical pattern with hapalindole U (C10S, 11R, 12R, and 15S), which is likely to be the common precursor to ambiguines. In the ambiguity-producing strain *F. ambigua* UTEX 1903, FamC1 is known to generate 12-*epi*-hapalindole U (**3a**). It is important to note that Dethe and coworkers recently reported the structure of synthetic (-)-12-*epi*-hapalindole U,<sup>[11]</sup> and our optical rotation of (+)-8.3 is consistent with the stereochemistry of natural product 12-*epi*-hapalindole U as C10S, 11R, 12S, and 15S. As expected, the product of FamC1 was reconfigured to hapalindole U (**2a**) by

adding FamC4 (**Figure 4**). Identical results were observed with homologs FilC1-FilC4 and FimC1-FimC4. Moreover, further screening in cyclase cross-pairing experiments revealed that FamC3/FilC3 can also alter the product of FamC1/FilC1 to Hapalindole U, albeit with lower efficiency than FamC4/FilC4 (**Figure 4**). Notably, the stereochemical alteration only occurred in the presence of excess  $\text{Ca}^{2+}$  (**Figure S12**). We note that hapalindole U production was independently reported by Liu et al.<sup>[6b]</sup> upon combining FamC1 with 10 equiv. of FamC4 and 20 mM  $\text{CaCl}_2$ . Our further titration study revealed that 0.5 mM  $\text{CaCl}_2$  is sufficient to fully activate 10  $\mu\text{M}$  of Stig cyclase, or alter product configuration in heterologous combinations of Fam cyclases (**Figure S13**).

In these two cases, we observed a distinct alteration in stereochemistry by adding another cyclase. FamC3, FamC4, and their homologs were initially observed to be cognate partners that appeared to be inactive independently. However, we further reasoned that the active sites of both cyclases may be engaged to cooperatively control hapalindole stereochemistry. To evaluate this hypothesis, we decided to prepare mutants, and compare Stig cyclase activity when one partner of a heterodimeric pair was catalytically inactivated by site-directed mutagenesis.<sup>[7a]</sup>

In our recent structural study of HpiC1, we probed the critical role of D214, an amino acid residue that is 100% conserved across all identified Stig cyclases and is the likely basis for acid catalyzed Cope rearrangement (**Figure S3**).<sup>[7a]</sup> By mutating this residue, HpiC1 activity was completely abrogated. Accordingly, this conserved residue was mutated to alanine, (FamC1-D214A, FamC2-D217A, FamC3-D214A, and FamC4-D215A), and each variant enzyme was confirmed to be inactive in the in vitro assay either as an individual cyclase or heterodimeric pair (**Figure S14**). Functional activity of the FamC3-D214A mutant was analyzed by incubating with wild-type FamC2 or FilC2 (**Figure 5**). We found that the catalytically inactive FamC3 mutant was no longer able to alter the product profiles; resulting in production of 12-*epi*-hapalindole H **5a** in both cases. Indeed, this is the same product obtained when an individual FamC2 or FilC2 enzyme is employed. Moreover, no alkaloid products were obtained when FamC2-D217A was combined with FamC3-wild-type or FamC3-D214A, indicating that FamC2 mediates an indispensable part of the catalytic reaction to form hapalindoles (**Figure S14**). Comparable results were obtained with mutants FamC1-D214A and FamC4-D215A, with reactions including FamC1-D214A failing to generate a product, while reaction with FamC1-wild-type and FamC4-D215A yielded 12-*epi*-hapalindole U (**3a**, **Figure 5**). Concordant results were observed with homologs WepC1-D214A and WepC2-D215A (**Figure S14**).

The experimental data described above are consistent with the hypothesis that a functional active site in FamC3 and FamC4 is required to cooperatively control the C-12 stereochemistry of hapalindoles. This insight also serves to identify the difference between FilC3 and FamC3, that despite sharing 98% identity with FamC3, FilC3 contains a six amino-acids insertion (NSVDIG) proximal to the active site, which is likely to alter the active site architecture (**Figure S15**), and thus influencing cyclase catalytic activity. We mutated FilC3 by deleting the extra six residues, and the enzymatic assay supported our hypothesis

that FilC3 $\Delta$ NSVDIG re-established its ability to alter FamC2 for production of Hapalindole H (**4a**); but interestingly, it did not change the product of FilC2 (**Figure 3**, **Figure 5**).

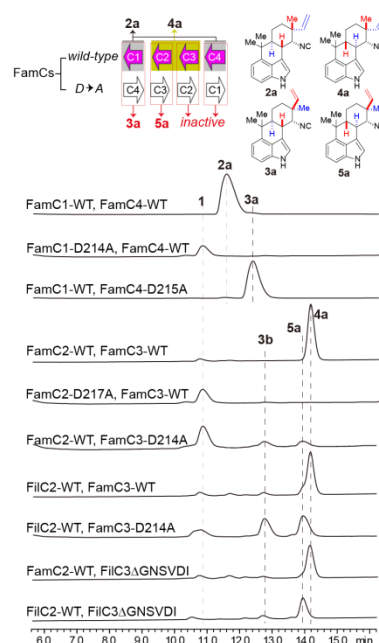


**Figure 5.** In vitro reactions of FamC1, FamC2, FamC3, FamC4 and select mutants with substrate **1** using 5 mM  $\text{CaCl}_2$ .

These data further support our hypothesis that FamC3, FamC4 and their homologs are engaged in hapalindole biosynthesis as subunits that combine for substrate catalysis in the Stig cyclase heteromeric pair. Interestingly, the products from the heteromeric pairs, hapalindole U (**2a**, FamC1-FamC4) and hapalindole H (**4a**, FamC2-FamC3), are reported natural metabolites from *F. ambigua* UTEX 1903. Thus, it is reasonable to conclude that such combinatorial pairing of Stig cyclases is biologically relevant to the intracellular environment. Another intriguing observation regarding the reconfiguration is that either **3a** (10*S*, 11*R*, 12*S*, 15*S*) to **2a** (10*S*, 11*R*, 12*R*, 15*S*), or **5a** (10*R*, 11*R*, 12*S*, 15*R*) to **4a** (10*R*, 11*R*, 12*R*, 15*R*) show alteration at the C-12 chiral center only, which is established during the Cope rearrangement step (**Figure 6**). The C-10 and C-15 chiral centers installed in the 6-*exo*-trig cyclization remain intact, along with the C-ring regiochemistry determined during terminal electrophilic aromatic substitution. A similar pattern was observed in the WepC1-WepC2 pair with a product change from **3a+3b** to **2a+2b**. These data suggest that the Cope rearrangement is singularly affected in the heteromeric Stig cyclase combinations. The 6-*exo*-trig cyclization and subsequent electrophilic aromatic substitution (or deprotonation to generate the tricyclic hapalindoles) are controlled by the independently active FamC1 and FamC2 and their homologs, which may be considered primary biocatalytic subunits as they are capable of functioning independently (**Figure 6**).

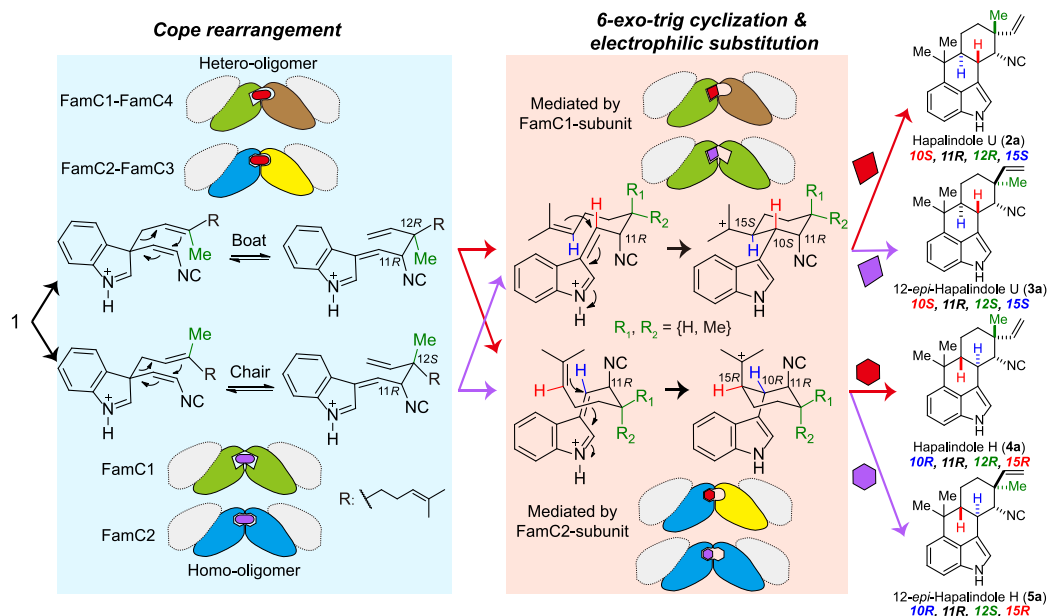


**Figure 6.** Proposed oligomeric model to form a combined cyclase active site for control of hapalindole stereochemistry. In this model, Cope rearrangement of substrate **1** is catalyzed by a combined active site to generate the C11 and C12 stereochemical pattern either via a boat conformation (hetero-oligomer FamC1-FamC4 (monomer is shown in green/khaki) and FamC2-FamC3 (cyan/yellow)) or via a chair conformation (homo-oligomer FamC1 and FamC2). The substrate is displayed as a red (boat; 12R) or purple (chair; 12S) oval in the combined active site. Both intermediates are transferred to the primary subunit (FamC1 or FamC2) to conduct the 6-*exo-trig* cyclization, where the oligomer comprising a FamC1-subunit (hetero-FamC1-FamC4 or homo-FamC1) generates the 10S/15S stereochemical pattern (diamond shape), while FamC2 forms 10R/15R (hexagon shape). Thus, four final intermediates are poised for the final electrophilic aromatic substitution to generate four products (**2a/3a/4a/5a**). We show a dashed-white monomer in each dimeric substructure to denote that the nature of the putative oligomeric cyclase structure (derived from homodimer or heterodimer) remains unknown.

Currently, we have demonstrated the importance of FamC3, FamC4 and their Stig cyclase homologs for control (with their cognate cyclase partners) of stereochemical induction during biogenesis of hapalindole core molecules. The precise molecular interactions involved to generate each of the known stereo- and regiochemical outcomes remains to be examined. Recent studies established the homodimeric conformation of HpiC1 by X-ray analysis,<sup>[7a, 7b]</sup> and biochemical evidence supports formation of Stig cyclase heterodimers, such as FamC2-FamC3.<sup>[6a]</sup> Based on the HpiC1 crystal structure and the high sequence homology of all Stig cyclases, we can deduce that the two active sites are too distant for a viable interaction in the dimeric state. Furthermore, based on the active site position and protein characteristics, we do not anticipate that a transient post-Cope intermediate could be readily transferred between distal active sites.<sup>[7a]</sup> However, if a higher order oligomer with at least two dimers is generated, an arrangement involving a joint active site derived from two distinct Stig cyclase subunits could be achieved (**Figure 6**).<sup>[12]</sup>

In our earlier studies, we observed that HpiC1 cannot produce Hapalindole U by pairing with HpiC4 or any other HpiC proteins, in contrast to FamC1-FamC4 (**Figure 7**). Moreover, we previously observed a form of HpiC1 with alternative crystal packing comprising a protein interface where the adjoining cyclase active sites are in direct contact (**Figure S16**). In this form bridging  $\text{Ca}^{2+}$  ions were observed at the interface suggesting that higher order oligomerization could be influenced

by  $\text{Ca}^{2+}$ .<sup>[7a]</sup> We further found that in the proposed oligomer-interface (residues 141-144), HpiC1 has different residues (EFQK) than FamC1 (TFKG), while both HpiC4 and FamC4 possess SKDI residues (**Figure S16**). We hypothesized that this disparity results in a variant oligomer form and active site interaction between HpiC1 and FamC1. To probe this further we generated two mutants HpiC1-TFKG<sub>141-144</sub> and FamC1-EFQK<sub>141-144</sub>, in an effort to interchange their activities by exchanging these corresponding interface residues. The enzymatic assay showed that FamC1-EFQK<sub>141-144</sub> failed to generate Hapalindole U by pairing with FamC4, while HpiC1-TFKG<sub>141-144</sub> gained the ability to produce Hapalindole U by interacting with HpiC4 (**Figure 7**). These results support our mechanistic hypothesis that Stig cyclases may function through formation of higher order oligomeric states.

Further work is still necessary to validate this hypothesis, as the FamC2-FamC3 hetero-oligomer and FamC1 homodimer do not require supplemental  $\text{Ca}^{2+}$  to function. In contrast, as shown above, the FamC1-FamC4 hetero-oligomer and WepC1 homodimer require excess levels of calcium. Taken together, these data indicate that the integrity of both active sites in the heteromeric cyclase associations is required to affect the stereochemical outcome of the Cope rearrangement, and the role of calcium in this process appears to be two-fold. First, with two integral sites in each protein subunit,  $\text{Ca}^{2+}$  is required for structural integrity and activity of Stig cyclases based on the HpiC1<sup>[7a]</sup> and FamC1<sup>[7b]</sup> crystal structure (and abrogation of

activity by EDTA). Second, calcium appears to also play a role in functional heteromeric or homo-oligomeric complexes to enable formation of a combined Stig cyclase active sites with resulting control of chiral induction at C-12 during the Cope rearrangement.

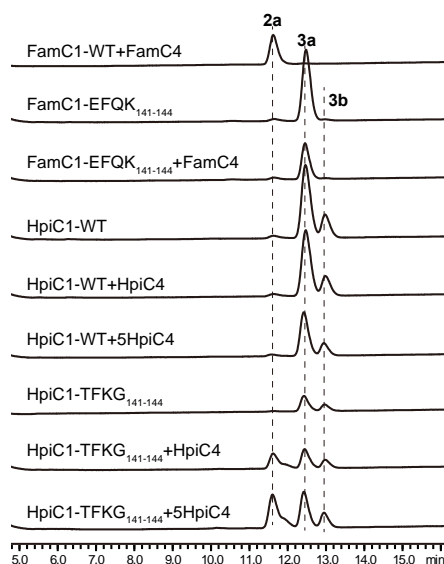


**Figure 7.** In vitro assay of FamC1 and HpiC1 mutants with substrate 1 and 5 mM of  $\text{CaCl}_2$ .

## Conclusion

In this study, we initially explored the enzymatic activity of Stig cyclases FilC2 and FilC3 to produce 12-*epi*-hapalindole H, which led to the discovery of  $\text{Ca}^{2+}$  as an important co-factor for functional Stig cyclases. Further interrogation with homologs FamC2 and FamC3 demonstrated that the product of FamC2 alone is 12-*epi*-hapalindole H. However, when FamC2 is combined with FamC3 the heteromeric complex specifically generates hapalindole H. This unexpected catalytic function of FamC3 was further observed in FamC4 (and its homologs FamC4/WepC2/FilC4/FimC4). In this case, the original 12-*epi*-hapalindole U metabolite of FamC1/WepC1/FilC1/FimC1, respectively, can be redirected to hapalindole U when combined with its cognate partner and supplemental (5mM)  $\text{CaCl}_2$ . Mutational analysis of the active site residue (D214A) with FamC cyclases and FilC3 $\Delta$ NSVDIG supported our hypothesis that FamC3, FamC4 and their homologs are cooperating to control the stereochemistry of hapalindole products through  $\text{Ca}^{2+}$ -promoted heteromeric pairing with cognate Stig cyclases. These biochemical observations are consistent with our recent HpiC1 crystal structure analysis that revealed Stig cyclases are capable of forming higher-order oligomers, and further reinforced by mutagenesis studies on FamC1 and HpiC1. Taken together, these functional and structural data provide a new proposal for stereocontrol in Stig cyclases. Our data indicate that as a first step, the Cope rearrangement is mediated by a combined active site comprised of heteromeric cyclase complexes. Next, the Cope rearrangement product shifts to the dominant cyclase

monomer to complete the 6-*exo-trig* cyclization and C-ring formation (**Figure 6**). Further structural and biochemical studies are in progress to verify the hetero-oligomeric complex formation and characterize additional stereochemical patterns (such as hapalindole J, and other predicted, but unidentified hapalindole/fischerindole metabolites (**Figure 1**) mediated by Stig cyclase biocatalysts.

## Acknowledgements

The authors thank the National Institutes of Health for financial support (R35 GM118101) as well as the National Science Foundation under the CCI Center for Selective C-H Functionalization (CHE- 1700982), and the Hans W. Vahiteich Professorship (to DHS). JO (UIC) thanks P01 CA125066 for supporting research on *Westiellopsis prolifica* SAG 16.93.

**Keywords:** Stig cyclase • hapalindole • oligomerization • biocatalysis • Cope rearrangement

- [1] a) R. E. Moore, C. Cheuk, G. M. L. Patterson, *J. Am. Chem. Soc.* **1984**, *106*, 6456-6457; b) V. Bhat, A. Dave, J. A. MacKay, V. H. Rawal, in *The Alkaloids: Chemistry and Biology*, Vol. 73 (Ed.: K. Hans-Joachim), Academic Press, San Diego, **2014**, pp. 65-160.
- [2] U. M. Acuña, S. Mo, J. Zi, J. Orjala, E. J. C. De Blanco, *Anticancer Res.* **2018**, *38*, 3299-3307.
- [3] K. Walton, M. Gantar, P. Gibbs, M. Schmale, J. Berry, *Toxins* **2014**, *6*, 3568-3581.
- [4] E. Cagide, P. G. Becher, M. C. Louzao, B. Espiña, M. R. Vieytes, F. Jüttner, L. M. Botana, *Chem. Res. Toxicol.* **2014**, *27*, 1696-1706.
- [5] a) S. Li, A. N. Lowell, F. Yu, A. Raveh, S. A. Newmister, N. Bair, J. M. Schaub, R. M. Williams, D. H. Sherman, *J. Am. Chem. Soc.* **2015**, *137*, 15366-15369; b) M. L. Hillwig, Q. Zhu, X. Liu, *ACS Chem. Biol.* **2014**, *9*, 372-377; c) M. L. Micallef, D. Sharma, B. M. Bunn, L. Gerwick, R. Viswanathan, M. C. Moffitt, *BMC Microbiol.* **2014**, *14*, 213-230; d) M. L. Hillwig, H. A. Fuhrman, K. Ittiamornkul, T. J. Sevco, D. H. Kwak, X. Liu, *ChemBioChem* **2014**, *15*, 665-669.
- [6] a) S. Li, A. N. Lowell, S. A. Newmister, F. Yu, R. M. Williams, D. H. Sherman, *Nat. Chem. Biol.* **2017**, *13*, 467-469; b) Q. Zhu, X. Liu, *Angew. Chem. Int. Ed. Engl.* **2017**, *56*, 9062-9066.
- [7] a) S. A. Newmister, S. Li, M. Garcia-Borrás, J. N. Sanders, S. Yang, A. N. Lowell, F. Yu, J. L. Smith, R. M. Williams, K. N. Houk, D. H. Sherman, *Nat. Chem. Biol.* **2018**, *14*, 345-351; b) C. C. Chen, X. Hu, X. Tang, Y. Yang, T. P. Ko, J. Gao, Y. Zheng, J. W. Huang, Z. Yu, L. Li, S. Han, N. Cai, Y. Zhang, W. Liu, R. T. Guo, *Angew. Chem. Int. Ed.* **2018**, *57*, 15060-15064; c) X. Tang, J. Xue, Y. Yang, T.-P. Ko, C.-Y. Chen, L. Dai, R.-T. Guo, Y. Zhang, C.-C. Chen, *RSC Adv.* **2019**, *9*, 13182-13185.
- [8] A. Raveh, S. Carmeli, *J. Nat. Prod.* **2007**, *70*, 196-201.
- [9] a) T. A. Smitka, R. Bonjouklian, L. Doolin, N. D. Jones, J. B. Deeter, W. Y. Yoshida, M. R. Prinsep, R. E. Moore, G. M. L. Patterson, *J. Org. Chem.* **1992**, *57*, 857-861; b) S. Mo, A. Krunic, G. Chlipala, J. Orjala, *J. Nat. Prod.* **2009**, *72*, 894-899.
- [10] a) Z. Lu, M. Yang, P. Chen, X. Xiong, A. Li, *Angew. Chem. Int. Ed.* **2014**, *53*, 13840-13844; b) D. Klein, D. Daloz, J. C. Braekman, L. Hoffmann, V. Demoulin, *J. Nat. Prod.* **1995**, *58*, 1781-1785; c) T. J. Maimone, Y. Ishihara, P. S. Baran, *Tetrahedron* **2015**, *71*, 3652-3665.
- [11] D. H. Dethe, S. Das, V. B. Kumar, N. A. Mir, *Chem.: Eur. J.* **2018**, *24*, 8980-8984.
- [12] a) J. Vonck, D. J. Mills, *Curr. Opin. Struct. Biol.* **2017**, *46*, 48-54; b) V. Villeret, B. Clantin, C. Tricot, C. Legrain, M. Roovers,

V. Stalon, N. Glansdorff, J. Van Beeumen, *Proc. Natl. Acad. Sci.* **1998**, *95*, 2801-2806.

Author Manuscript

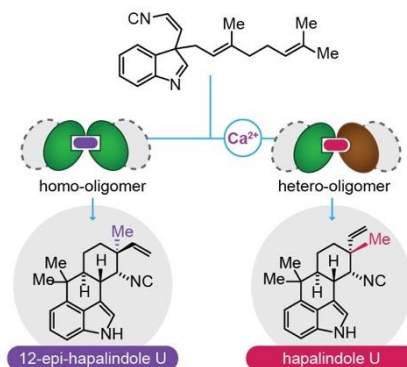


Entry for the Table of Contents (Please choose one layout)

Layout 1:

## RESEARCH ARTICLE

The stereochemical pattern of enzymatic product can be reconfigured by pairing with a homologous protein to form a hetero-oligomer which was induced by  $\text{Ca}^{2+}$ .



Shasha Li, Sean A. Newmister, Andrew N. Lowell, Jiachen Zi, Callie R. Chappell, Fengang Yu, Robert M. Hohlman, Jimmy Orjala, Robert M. Williams, and David H. Sherman\*

Page No. – Page No.

Control of stereoselectivity in diverse hapalindole metabolites is mediated by cofactor induced combinatorial pairing of Stig cyclases

Author Manuscript